Critical Mineral Resources in the Cornudas Mountains, Otero County, New Mexico.

Virginia T. McLemore, Nels Iverson, Mason Woodard, Snir Attia, and Evan J. Owen

2023, pp. 132-141. https://doi.org/10.56577/FFC-73.132

in:

Evaporite Karst of the Lower Pecos Region, Land, Lewis; Bou Jaoude, Issam; Hutchinson, Peter; Zeigler, Kate; Jakle, Anne; Van Der Werff, Brittney, New Mexico Geological Society 73 rd Annual Fall Field Conference Guidebook, 152 p. https://doi.org/10.56577/FFC-73

This page is intentionally left blank to maintain order of facing pages.

New Mexico Geological Society Guidebook, 73rd Fall Field Conference, 2023, p. 132–141, https://doi.org/10.56577/FFC-73.132

CRITICAL MINERAL RESOURCES IN THE CORNUDAS MOUNTAINS, OTERO COUNTY, NEW MEXICO

VIRGINIA T. MCLEMORE[1], NELS IVERSON[1], MASON WOODARD[1], SNIR ATTIA[1], AND EVAN J. OWEN[1]

[1]New Mexico Bureau of Geology and Mineral Resources, New Mexico Institute of Mining and Technology, Socorro, NM 87801; virginia.mclemore@nmt.edu

Abstract—Reexamination of the mineral resources in the Cornudas Mountains is warranted in light of today's economic importance of critical minerals that are essential in most of our electronic devices. The Cornudas Mountains form the northern Trans-Pecos alkaline magmatic province in the southern part of the North American Cordilleran alkaline-igneous belt. New mapping, petrography, $^{40}Ar/^{39}Ar$ geochronology, and geochemical analyses have provided a better understanding of the emplacement of the intrusions and associated mineral deposits in the area. The igneous rocks in the Cornudas Mountains were emplaced into Permian and Cretaceous sedimentary rocks in two pulses at 37.14–34.5 and 32.48–26.95 Ma, just prior to or during the early phases of Rio Grande Rift extension, and consist of (1) larger nepheline syenite–syenite laccoliths and plugs, (2) phonolite plugs, sills, and dikes, (3) smaller syenite plugs and dikes, and (4) volcanic breccia dikes. New U.S. Geological Survey geophysical data indicate that some of the larger intrusions extend into the subsurface as pipe-like geometries, with additional buried intrusions potentially at depth that could be additional exploration targets. The focus of exploration for critical minerals in the Cornudas Mountains is for rare earth elements (REE), niobium (Nb), and zirconium (Zr) that are found within (1) the basal unit (PEnsp2) of the Wind Mountain nepheline syenite laccolith, (2) syenite-phonolite and volcanic breccia dikes and plugs, and (3) skarns and carbonate-replacement deposits in Chess Draw and Wind Mountain areas. Some samples contain as much as 3110 ppm total REE. REE could be leached from a mineral concentrate of REE-bearing minerals (eudialyte, zircon, monazite, bastnäsite, calciocatapleiite, vitusite, roumaite, xenotime). Pyrochlore (Nb), eudialyte (Zr), and zircon (Zr) are also found with the REE-bearing minerals and have potential for economic recovery. Another potential mineral resource is nepheline syenite for use as ceramics, glass, or other industrial use.

INTRODUCTION

Although the definition of a critical mineral varies from country to country depending on supply, demand, and strategic conditions, critical minerals in the United States are defined as nonfuel mineral commodities that are essential to the economic and national security of the United States and are from a supply chain that is vulnerable to global and national disruption. In the mining industry, a *mineral* refers to any rock, mineral, or other naturally occurring material of economic value and sold as a commodity. There are currently 53 minerals listed as critical for the United States (Committee on Critical Mineral Impacts of the U.S. Economy, 2008; McLemore and Gysi, 2023), including rare earth elements (REE), niobium (Nb), and zirconium (Zr). REE include the 15 lanthanide elements (La, Ce, Pr, Nd, Pm, Sm, Eu, Gd, Tb, Dy, Ho, Er, Tm, Yb, Lu, atomic numbers 57–71), yttrium (Y), and scandium (Sc).

The focus of exploration for critical minerals in the Cornudas Mountains is for REE, Zr, and Nb (Schreiner, 1994; Nutt et al., 1997; Nutt and O'Neill, 1998; McLemore, 2018; McLemore et al., 2022). REE are used in magnets and batteries, and Ce is an important polishing agent. Other uses include the manufacture of wind turbines, solar panels, magnetic refrigeration, and more efficient light bulbs. Zirconium is used as a refractory material in laboratory crucibles and metallurgical furnaces and as an abrasive. Niobium is used in superconductors, batteries, and alloys. REE, Zr, and Nb resources are located in New Mexico (McLemore, 2014, 2018), but these deposits have not been important exploration targets in the past because demand has been met elsewhere. However, with the projected increase in demand for critical minerals and the potential lack of available production from China, New Mexico deposits are being reexamined for their economic potential. Another potential resource in the Cornudas Mountains is the use of nepheline syenite in ceramics, glass, or other industrial applications (McLemore et al., 1994; McLemore and Guilinger, 1993, 1996).

The Cornudas Mountains intrusive center is located along the North American Cordilleran alkaline-igneous belt in southern New Mexico and northern Texas (Figs. 1, 2; McLemore, 2018) and form the northern extent of the Trans-Pecos alkaline magmatic province (Barker, 1977, 1987). This study focuses on a reexamination of the geology and mineral-resource potential of the Cornudas Mountains and is a summary of McLemore et al. (2022), which includes new detailed geologic, geochemistry, mineralogical, and geochronological descriptions and supporting data.

METHODS OF STUDY

Geologic mapping of the Cornudas Mountains was conducted by the authors at scales ranging from 1:1,000 to 1:24,000 between 2020 and 2022 (McLemore et al., 2022). Previous geologic maps aided in the new mapping (Clabaugh, 1941; Zapp, 1941; Timm, 1941; Warner et al., 1959; Schreiner, 1994; U.S. Borax, 1986; McLemore, 1996; Nutt et al., 1997; O'Neill and Nutt, 1998). Drill core from past exploration efforts were examined, and selected samples were collected for study. Unaltered igneous intrusions and mineralized samples were collected for geochronological, mineralogical, and geochemical analyses. Mineralized areas were previously sampled and analyzed in 1980 and 2009–2010 by McLemore and in 1995 by the U.S. Bureau of Mines (Schreiner, 1994). These previous studies concluded that the deposits were not economic at that time. In 2016, Geovic began new exploration in the area in light of the recent change in economics and importance of REE and other critical minerals. These chemical data were combined, reported in McLemore et al. (2022, appendix 4), and used in geochemical interpretations.

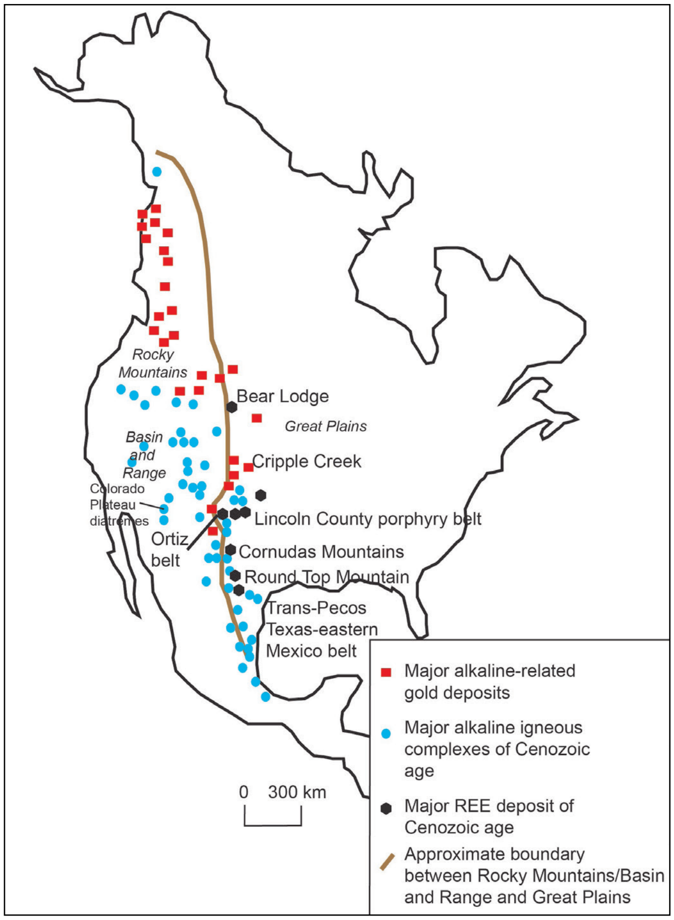

FIGURE 1. Simplified map showing the extent of the North American Cordilleran alkaline-igneous belt (modified from Mutschler et al., 1985, 1991; McLemore, 1996, 2018).

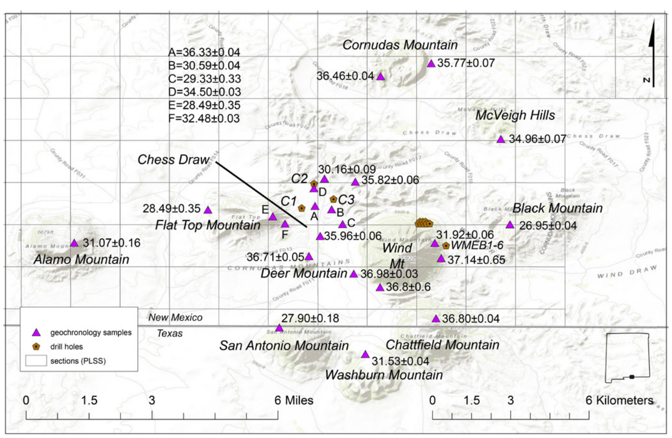

FIGURE 2. Intrusive bodies in the Cornudas Mountains, showing location of geochronology samples and drill holes. Summarized in Table 1.

GEOLOGIC SETTING OF THE CORNUDAS MOUNTAINS

The oldest rocks in the Cornudas Mountains are Permian limestones of the Hueco, Yeso, and San Andres formations and Cretaceous sedimentary rocks of the Campagrande Formation, Cox Sandstone, and Muleros-Mesilla Valley formations. Dikes, sills, and laccoliths of varying compositions, ages, and dimensions intruded the Permian and Cretaceous sedimentary rocks (Table 1). Quaternary surficial deposits are found along drainages and slopes in the Cornudas Mountains. Map units are defined in Table 1 and McLemore et al. (2022).

^{40}AR/^{39}AR GEOCHRONOLGY RESULTS

The emplacement ages of the Cornudas Mountains intrusions have been previously understudied. Prior to this study, only six of the intrusions had been dated, focusing on Wind Mountain and intrusions in Chess Draw. Only one of the ages was done using high-precision ^{40}Ar/^{39}Ar geochronology. These data show a range of ages from 38.6–31.6 Ma (Table 1; Fig. 3).

To better understand the emplacement history of the Cornudas Mountains, 21 different intrusions were dated using the ^{40}Ar/^{39}Ar dating method (Table 1; Figs. 2, 3). In total, 27 samples were dated, some with two aliquots, and they display a range of age spectra complexities from alteration or ^{40}Ar loss, excess ^{40}Ar, and/or ^{39}Ar recoil (McLemore et al., 2022).

All ages are considered to be minimum emplacement ages, as textural and field relationships do not suggest any of the igneous rocks were erupted subaerially. Some of the intrusions were dated using multiple materials (biotite, amphibole, and groundmass concentrate) to assess cooling history that may be present because of closure temperature differences between mineral phases. Comprehensive geochronology presented in McLemore et al. (2022) shows that igneous rocks were emplaced in two pulses at 37.14–34.50 and 32.48–26.95 Ma (Fig. 3), just prior to or during the earliest phases of Rio Grande Rift extension, spanning a longer interval than that recorded by the previously published K/Ar ages (36.0–31.6 Ma). Two sigma errors for the individual ages are in Table 1.

DESCRIPTION OF IGNEOUS ROCKS

The igneous rocks in the Cornudas Mountains intruded Permian and Cretaceous sedimentary rocks and consist of (1) larger nepheline syenite to syenite laccoliths, (2) phonolite and nepheline syenite sills, (3) smaller syenite to nepheline syenite intrusions in Chess Draw, and (4) numerous syenite, nepheline syenite, volcanic breccia, and phonolite dikes (Table 1, Fig. 2). Other dikes, sills, and plugs are buried by sedimentary cover, as indicated by subsurface drilling (King and Harder, 1985; McLemore et al., 2023), geophysical surveys (Bultman, 2021a, b, 2022), and are suggested by structural anomalies (i.e., folds, synclines, faults; Nutt et al., 1997; O'Neill and Nutt, 1998) in the overlying sedimentary rocks. The geophysical surveys indicate that the intrusions in the Cornudas Mountains are vertical pipes and most of the sills have no magnetic expression

(Bultman, 2021a, b, 2022). Several intrusions are buried with no intrusions found at the surface, which offer new exploration targets (Bultman, 2021a, b, 2022).

Geochemically, the igneous rocks in the Cornudas Mountains are similar in composition, regardless of age and form (McLemore et al., 2022). They are ferroan, alkali-calcic to alkali (according to diagrams by Frost et al., 2001) and metaluminous to peraluminous (McLemore et al., 2022). Most igneous rocks exhibit light-REE-enriched, chondrite-normalized REE patterns with a strong negative Eu anomaly. The negative Eu anomaly indicates feldspar fractionation. Geochemical plots are included in the road log section of this guidebook (Owen and McLemore, this guidebook) and McLemore et al. (2022). The following is a description of the igneous intrusions.

Wind Mountain

The Wind Mountain laccolith is the oldest intrusion in the Cornudas Mountains (37.14±0.65 Ma) and consists of six mineralogical and textural zones (Table 2, Fig. 4; McLemore, 1996, 2022; McLemore and Guilinger, 1996). The margin of the laccolith is foliated and dips steeply away from the center of the intrusive body. The laccolith is typically gray to cream colored and weathers to darker colors, consisting of albite and alkali feldspars, nepheline, biotite, and a variety of accessory minerals. Varying amounts of pyroxene (aegirine-augite to aegirine to diopside-hedenbergite) and amphibole (arfvedsonite) minerals form dark-colored aggregates dispersed throughout the rock. Locally, the nepheline syenite is red in color due to the abundance of eudialyte and other Zr- and REE-bearing

TABLE 1. Intrusive bodies in the Cornudas Mountains, locations shown in Figure 2 (modified from Barker et al., 1977; McLemore, 2018; new mapping). Details of the geochronology are provided in McLemore et al. (2022). Map units defined by McLemore et al. (2022). *Note that fragments of phonolite are found in the Chattfield Mountain sill, indicating an older phonolite not identified at the surface.

Locality, map unit	Predominant lithology	Form	Thickness (km)	Sample No. or reference for age date	Age (Ma)
Wind Mountain, PEnsp2	Nepheline syenite to syenite porphyry	Layered laccolith	0.25	McLemore (1996), CORN814	36.8±0.6, 37.14±0.65
Lil' Windy (west Wind Mountain), PEnsp3	Nepheline syenite	Laccolith	0.1	CORN4005	36.98±0.03
Chattfield Mountain, PEp*	Phonolite	Sill	0.15	CORN4015	36.80±0.04
Deer Mountain (Little Wind Mountain), PEns, PEm	Nepheline syenite	Laccolith	0.1	CORN2000	36.71±0.05
Sill west of Cornudas Mountain, PEp	Quartz syenite to syenite	Sill	0.1	CORN4019	36.46±0.04
Northwest Chess Draw augite syenite, PEas (Tas of Potter, 1996a, b), surrounded by PEs	Augite syenite inner zone, syenite outer zone, intruded by phonolite dike	Plug	0.1	CORN177	36.33±0.04
South Chess Draw nepheline syenite, PEnsc	Nepheline syenite	Sill	0.02	CORN20-10	35.96±0.06
Chess Draw, PEbx	Volcanic breccia	Dikes	0.01	nd	nd
Dike north of Wind Mountain, PEp	Phonolite	Dike	0.01	CORN181	35.82±0.06
Cornudas Mountain, PEqs, PEs	Quartz syenite to syenite	Plug or laccolith, sill	0.1	CORN112	35.77±0.07
McVeigh Hills, PEs, PEqs	Quartz syenite to syenite	Top of a laccolith or sill?	?	CORN226	34.96±0.07
Mesquite Hill (north Chess Draw), PEp	Phonolite	Dike	0.01	CORN4008	34.50±0.03
Dike east of Flat Top, PEp	Phonolite	Dike	0.01	CORN117	32.48±0.03
Wind Mountain dike, PEp	Phonolite	Dike	0.01	CORN805	31.92±0.06
Washburn Mountain, PEns	Nepheline syenite	Sill	0.15	CND208	31.53±0.44
Alamo Mountain, PEp, PEm	Phonolite	Discordant sheet or sill	0.25	CORN4002	31.07±0.16
Northeast Chess Draw (unnamed hill), PEpp	Phonolite	Plug	0.1	CORN4006	30.59±0.04
Chess Draw dike, PEp	Phonolite	Plug	0.01	CORN4007	30.16±0.09
East Chess Draw nepheline syenite, PEnsc	Nepheline syenite	Plug	0.01	CORN79	29.33±0.23
Flat Top, PEp	Phonolite	Sill (50–75 ft thick)	0.015–0.023	CORN4004	28.49±0.35
San Antonio Mountain, PEns	Nepheline syenite	Laccolith	0.15	CORN4013	27.90±0.18
Black Mountain, PEps	Nepheline syenite	Sill	0.07	CORN4011	26.95±0.04

minerals. Geophysical data indicate it is a near vertical pipe in geometry (Bultman, 2021a, b, 2022).

Chattfield Mountain (PEp)

Chattfield Mountain (36.8±0.04 Ma) is formed by a dark green to black, aphanitic phonolite sill or laccolith (Tables 1, 3) and consists of aegirine-augite, anorthoclase, albite, analcime, nepheline, and minor arfvedsonite and titanomagnetite. The fine-grained matrix locally has a trachytic texture formed by anorthoclase. Small fragments of phonolite are found in the sill, indicating older phonolite intrusions at depth. There is no geophysical anomaly associated with this intrusion (Bultman, 2021a, b, 2022).

Deer Mountain (PEns, PEm)

Deer Mountain (36.67±0.04 Ma) laccolith is in the southern portion of Chess Draw and consists of light gray to pinkish-gray, coarse- to fine-grained, equigranular analcime nepheline syenite to syenite with nepheline, analcime, aegirine-augite, pyroxene, perthitic feldspar, and albite with minor amounts of biotite, apatite, calcite, and titanite. The nepheline syenite comprising Deer Mountain does not appear to vary in mineralogical or chemical composition, although a finer-grained border facies (PEm) is present locally along the western margin (McLemore et al., 2022). Geophysical data indicate it is a near vertical pipe in geometry (Bultman, 2021a, b, 2022).

Chess Draw Intrusions

The Chess Draw area spatially includes the southern Chess Draw area between Wind and Flat Top Mountains (Fig. 2) and includes numerous phonolite (PEp), syenite (PEs), trachyte (PEt), nepheline syenite (PEns), and volcanic breccia (PEbx) plugs, sills, and dikes (Tables 1, 3; McLemore et al., 2022). The intrusions are discussed in more detail in McLemore et al. (2022) and summarized in Table 1. The ages of the intrusions in Chess Draw range from 36.33±0.04 to 29.33±0.23 Ma. There are two magnetic anomalies in the geophysical data suggesting that these intrusions form the top of buried laccoliths

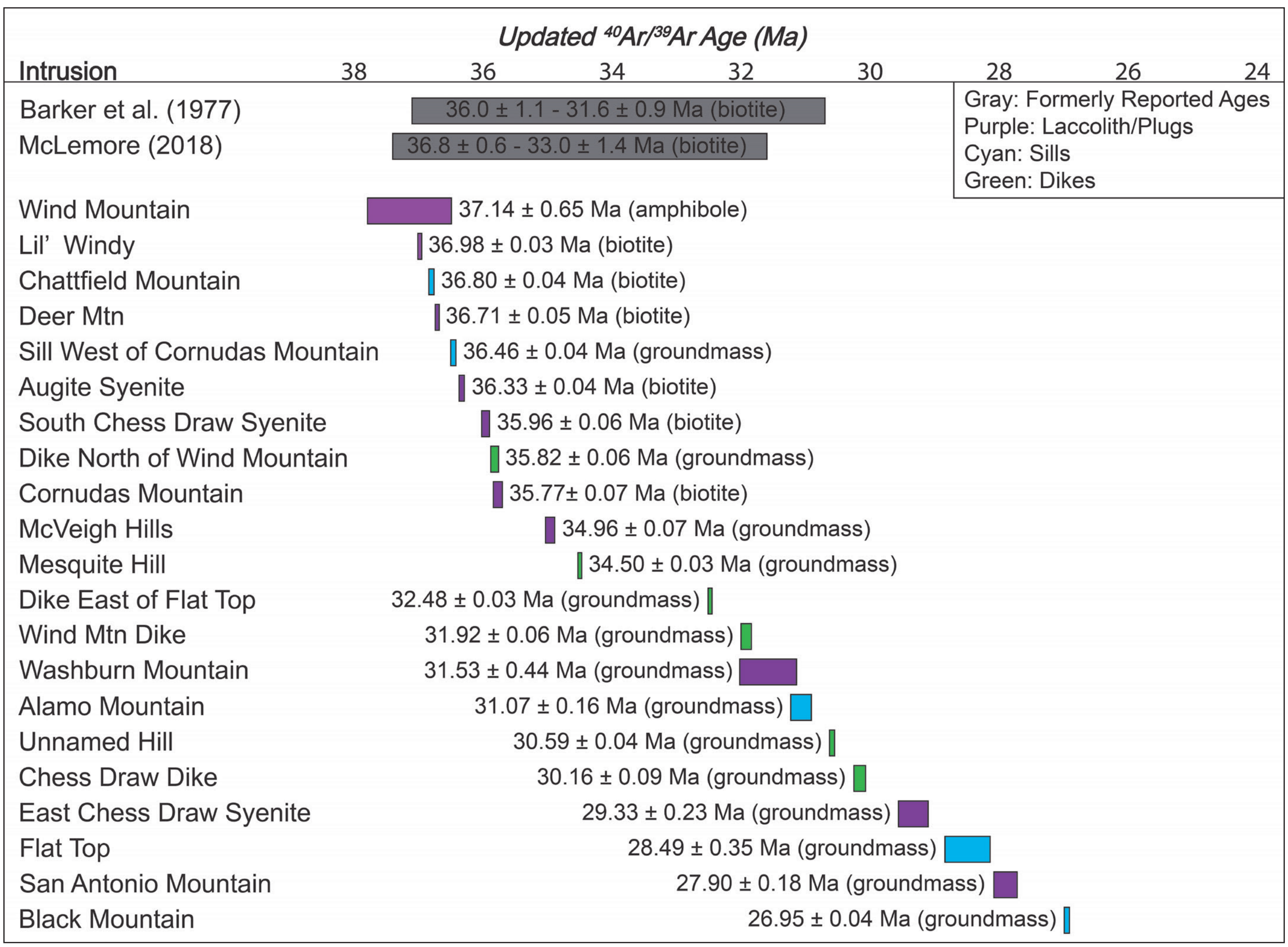

FIGURE 3. Summary view of new $^{40}Ar/^{39}Ar$ data (colored bars) and published data (gray bars from Barker et al., 1977 and McLemore, 2018). Colored bars denote the type of intrusion (purple are laccoliths and plugs, blue are sills, and green are dikes), and the length of the bar represents the precision of the age. Most intrusions do not overlap in time, and there is no spatial or temporal relationship in the timing and type of intrusion for the Cornudas Mountains in New Mexico.

TABLE 2. Description of the textural units comprising the Wind Mountain laccolith (modified from P. Graseah, field mapping, July 1992, published in McLemore and Guilinger, 1993). Cross section is shown in Figure 4.

Map symbol	Name	Description	Comments
PEspfg1	Syenite porphyry	Fine grained, contains minor analcime, aegirine, Na amphibole, biotite, and magnetite in a plagioclase-rich groundmass	Top of laccolith
PEspfg2	Syenite porphyry	Fine grained, contains predominant plagioclase, aegirite, Na amphibole, biotite	
PEspfg3	Syenite porphyry	Fine grained, contains predominant plagioclase, aegirite, Na amphibole, biotite but is more mafic than Tspfg2	
PEspfg4	Syenite porphyry	Fine grained, contains analcime, aegirite, Na amphibole, biotite, and magnetite in a plagioclase-rich groundmass	
PEnsp1	Nepheline syenite porphyry	Coarse grained, contains K-feldspar phenocrysts in a matrix of plagioclase, nepheline, analcime, with accessory aegirine, Na amphibole, minor magnetite	
PEnsp2	Nepheline syenite porphyry	Medium grained, contains K-feldspar phenocrysts in a matrix of plagioclase, nepheline, minor analcime, with accessory aegirine, Na amphibole, minor magnetite	Base of laccolith
PEnsp3 (Lil' Windy)	Nepheline syenite porphyry	Medium grained, contains blocky, vertical K-feldspar phenocrysts in a matrix of plagioclase, nepheline, with accessory arfvedsonite-aegerite, minor magnetite	Hill southwest of Wind Mountain

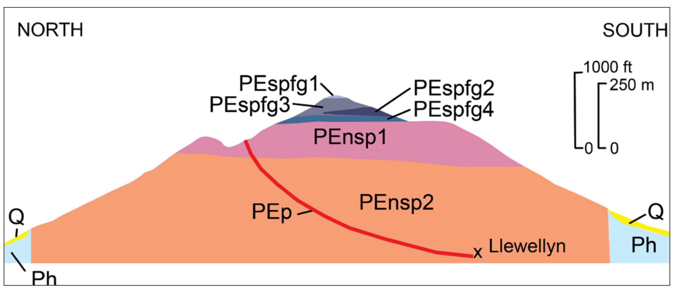

FIGURE 4. North-south cross section of Wind Mountain laccolith (McLemore et al., 2022). See Table 2 and McLemore et al. (2022) for description of units. Llewellyn is a prospect (symbol x).

(Bultman, 2021a, b, 2022). The abundance of volcanic breccia dikes supports this interpretation.

Cornudas Mountain (PEqs/PEs)

Cornudas Mountain laccolith is the northernmost of the intrusions, is medium gray, weakly foliated, granoblastic to porphyritic, fine- to medium-grained syenite (PEs) to quartz-syenite (PEqs), and is 35.77±0.07 Ma. The rocks consist of tabular, euhedral anorthoclase, subhedral aegirine-augite, biotite, arfvedsonite, and local interstitial quartz, apatite, and anatase. Additional outcrops of quartz syenite are exposed east of the Cornudas Mountains (some are dikes) and are surrounded by limestone beds. A 15 m thick sill intrudes the limestone west of Cornudas Mountain. Geophysical data suggest that this laccolith is the northwestern part of a larger intrusion or group of intrusions at depth that extends toward McVeigh Hills and Black Mountain (Bultman, 2021a, b, 2022).

McVeigh Hills (PEs, PEqs)

Previously unmapped, small intrusions of syenite (PEs) to quartz syenite (PEqs) to nepheline syenite (PEns) are in the McVeigh Hills and are intruded by phonolite (Fig. 2). The syenite to quartz syenite to nepheline syenite is 34.96±0.07 Ma and are medium gray to orange, weakly foliated, granoblastic to porphyritic, fine to medium grained. The rocks consist of anorthoclase, subhedral clinopyroxene, biotite, and interstitial quartz. Phonolite dikes intrude the syenite. McVeigh Hills lies on top of an extensive magnetic high spanning from Cornudas Mountain southeast toward Black Mountain (Bultman, 2021a, b, 2022).

Washburn Mountain (PEns)

The nepheline syenite sill that forms Washburn Mountain is 31.53±0.44 Ma, dark gray, and consists of anorthoclase, nepheline, aegirine-augite, and altered arfvedsonite. Locally, a porphyritic texture is formed by large anorthoclase phenocrysts up to 2–3 cm long. Geophysical data indicate it is a series of near vertical pipes or dikes in geometry (Bultman, 2021a, b, 2022).

Alamo Mountain (PEp)

Alamo Mountain (31.07±0.16 Ma) consists of a medium gray to dark green, aphanitic, foliated phonolite sill or laccolith with well-developed magmatic foliation, locally displaying trachytic texture. On western and southern flanks of Alamo Mountain (PEp), the phonolite is platy with foliation dipping at a low angle relative to underlying sedimentary bedding. There is no geophysical anomaly associated with this intrusion (Bultman, 2021a, b, 2022).

Flat Top Mountain (PEp)

Flat Top Mountain is capped by one to four sills that are 15–23 m thick, black to dark green, fine-grained phonolite (PEp) that is 28±0.35 Ma. Trachytic to porphyritic texture is locally found and consists of feldspar, aegirine, and analcime.

TABLE 3. $^{40}Ar/^{39}Ar$ ages from the Cornudas Mountains. MSWD is Mean Square of the Weighted Deviates and is the parameter used to assess the goodness of fit of the calculated line to the data.

Sample	Unit	Material	Age Type	N	MSWD	Age (Ma)	±2σ	Comments
CORN2000	Deer Mtn.	Amphibole	Plateau	10/14	1.8	36.67	0.04	
CORN112	Cornudas Mtn.	Biotite	Isochron	8/12	467.6	35.77	0.07	High MSWD indicates excess ^{40}Ar
CORN805	Wind Mtn. Dike	Groundmass	Plateau	5/10	2.6	31.92	0.06	High MSWD from argon loss in first few steps
CORN814	Wind Mtn.	Amphibole	Isochron	12/14	2.8	37.14	0.65	High MSWD from argon loss in first few steps
CORN4005	Lil' Windy	Biotite	Isochron	12/12	34.7	36.98	0.03	High MSWD
CORN4006	Unnamed Hill	Groundmass	Isochron	10/10	90.0	30.59	0.04	High MSWD from argon loss in first few steps
CORN4007	Phonolite Dike	Groundmass	Plateau	7/10	0.9	30.16	0.09	
CORN4008	Mesquite Hill	Groundmass	Isochron	10/10	28.9	34.50	0.03	High MSWD indicates excess ^{40}Ar
CORN4002	Alamo Mtn.	Groundmass	Plateau	5/10	1.9	31.07	0.16	High MSWD from argon loss in first few steps and scatter due to recoil
CORN177	Augite Syenite	Biotite	Plateau	4/13	0.0	36.33	0.04	Contains excess ^{40}Ar
CORN20-10	S. Chess Draw Dike	Biotite	Plateau	5/13	2.1	35.93	0.06	High MSWD from argon loss in first few steps
CORN4015	Chatfield Mtn.	Biotite	Plateau	9/13	0.6	36.80	0.04	Contains excess ^{40}Ar
CORN4019	Sill W. of Cornudas	Groundmass	Isochron	10/10	108.4	36.46	0.04	High MSWD and spectra shape indicates excess ^{40}Ar
CORN79	E. Chest Draw Dike	Groundmass	Plateau	6/10	2.0	29.39	0.22	Argon loss in first few steps
CORN117	Dike E. of Flat Top	Groundmass	Plateau	6/10	0.9	32.48	0.03	High MSWD from argon loss in first few steps and scatter due to recoil
CORN181	Dike N. of Wind Mtn.	Groundmass	Isochron	6/10	26.4	35.82	0.06	High MSWD from argon loss in first few steps
CND-208	Washburn Mtn.	Groundmass	Isochron	9/10	30.5	31.53	0.44	Climbing spectra and short plateau
CORN226	McVeigh Hills	Groundmass	Plateau	4/10	2.5	34.96	0.07	High MSWD from argon loss in first few steps and scatter due to recoil
CORN4004	Flat Top	Groundmass	Plateau	4/10	1.9	28.49	0.35	
CORN4011	Black Mtn.	Groundmass	Plateau	3/10	1.6	26.95	0.04	Argon loss in first few steps
CORN4013	San Antonio	Groundmass	Plateau	4/10	1.5	28.26	0.21	Argon loss in first few steps

Phonolite dikes intrude the underlying limestone on the south, southeast, east, and north flanks (McLemore et al., 2022). There is no geophysical anomaly associated with this intrusion (Bultman, 2021a, b, 2022).

San Antonio Mountain (PEns)

San Antonio Mountain (28.26±0.21 Ma) consists of a gray, fine-grained, holocrystalline, porphyritic nepheline syenite, with local diabasic texture. The nepheline syenite consists of microcline or anorthoclase, nepheline, aegirine-augite, arfvedsonite, and hematite, with accessory aenigmatite, fayalite, titanomagnetite, and monazite. Geophysical data indicate it is a near vertical pipes in geometry (Bultman, 2021a, b, 2022).

Black Mountain (PEps)

Black Mountain is the youngest of the intrusions (26.95±0.04 Ma) and consists of dark gray to gray-green, porphyritic, foliated, fine- to medium-grained nepheline syenite sills. Phenocrysts consist of euhedral anorthoclase up to 2–3 cm long in groundmass of anorthoclase, clinopyroxene, biotite, nepheline, and analcime, with local trace eudialyte. Black Mountain is part of the Cornudas–McVeigh Hills geophysical anomaly (Bultman, 2021a, b, 2022).

TABLE 4. REE-Zr-Nb minerals found in the Cornudas Mountains. *Confirmed by NMBGMR thin section, XRD (McLemore et al., 2022, appendix 6) or electron microprobe (McLemore et al., 2022, appendix 8). Additional references include DeMark (1989). na = not analyzed. ? = confirmation of the mineral species is required.

Mineral	Occurrence	Chemical formulae	Approximate amount of total REE (wt%)	Reference
*Aqualite (Eudialyte group)	Skarn north of Wind Mountain (CORN104)	$(H_3O)_8(Na,K,Sr)_5Ca_6Zr_3Si_{26}O_{66})(OH)_9Cl$	9	McLemore et al. (2022)
*Bastnäsite	Hexagonal crystals, disseminated in nepheline syenite	$(Ce,La)(CO_3)F$	66	McLemore et al. (2022)
Brockite	Vugs in nepheline syenite	$(Ca,Th,Ce)PO_4 \bullet H_2O$	6	Mindat.Org
*Catapleiite (calciocatapleiite)	Miarolitic cavities, platy to tabular, disseminated in nepheline syenite	$Na_2Zr(Si_3O_9) \bullet 2H_2O$	2	Boggs (1985)
Elpidite	Prismatic, in miarolitic cavities	$Na_2ZrSi_6O_{15} \bullet 3H_2O$	na	Michayluk and Cone (2017b)
Epididmite	Psuedohexagonal plates	$Na_2Be_2Si_6O_{15} \bullet H_2O$	na	Michayluk and Cone (2017b)
*Eudialyte	Dikes, sills, and laccoliths and in miarolitic cavities	$Na_4(Ca, Ce)_2(Fe^{2+}, Mn^{2+})$ $YZrSi_8O_{22}(OH,Cl)_2$	9	Barker and Hodges (1977), Clabaugh (1950), Boggs (1985, 1987)
*Fluorite	Breccia, skarns	CaF_2	?	Barker et al. (1977), Schreiner (1994)
Gaidonnayite	Miarolitic cavities	$Na_2Zr(Si_3O_9) \bullet 2H_2O$	?	Michayluk and Cone (2017b)
*Galena	Dikes, nepheline syenite Wind Mountain	PbS	na	Schreiner (1994), McLemore et al. (2022)
*Georgechaoite	Miarolitic cavities, coatings on microcline or acmite, from south side of Wind Mountain	$NaKZrSi_3O_9 \bullet 2H_2O$	na	Boggs (1985), Boggs and Ghose (1985), Ghose and Thakur (1985)
*Hydroxy-manganopyrochlore	Phonolite dike	$(Mn^{2+},Th,Na,Ca,REE)_2(Nb,Ti)_2O_6(OH)$	na	McLemore et al. (2022)
*Lueshite	Phonolite dike	$NaNbO_3$	na	McLemore et al. (2022)
*Maganoeudialyte	Skarn east of Wind Mountain (CORN108), nepheline syenite Wind Mountain	$Na_{14}Ca_6Mn_3Zr_3[Si_{26}O_{72}(OH)_2]$ $(H_2O,Cl,O,OH)_6$	9	McLemore et al. (2022)
*Molybdenite	Disseminated in nepheline syenite	MoS_2	na	Michayluk and Cone (2017a)
*Monazite	Miarolitic cavities, disseminated in nepheline syenite, skarns	$Ce, La, Nd(PO_4)$	65	Boggs (1985)
Niobian rutile	Vugs, miarolitic cavities	$(Ti,Nb)O_2$	na	Schreiner (1994)
*Oxynatropyrochlore (Pyrochlore group)	skarn	$(Na,Ca,U)_2Nb_2O_6(O,OH)$	na	McLemore et al. (2022)
Parakeldyshite	Nepheline syenite, Wind Mountain	$Na_2ZrSi_2O_7$	na	McLemore (1996)
*Parasite-Ce	Disseminated nepheline syenite	$CaCe_2(CO_3)_3F_2$	61	Michayluk and Cone (2017b)
*Pyrite	Within mineral aggregates of ferromagnesian minerals in syenite dike and skarn in Chess Draw, Wind Mountain nepheline syenite	FeS_2	na	Schreiner (1994), McLemore et al. (2022)
*Pyrochlore	Nepheline syenite	$(Na,Ca)_2Nb_2O_6(OH,F)$	na	This study
*Rheniite?	In Wind Mountain nepheline syenite (CORN812)	ReS_2	na	This study, needs confirmation but sample contains 0.002 ppm Re (higher than most)
*Roumaite	In Wind Mountain nepheline syenite (CORN260)	$(Ca,Na,REE)_7(Nb,Ti)[Si_2O_7]_2OF_3$	7–10	McLemore et al. (2022)
*Sergevanite (eudialyte group)	Nepheline syenite	$Na_{15}(Ca_3Mn_3)(Na_2Fe)Zr_3Si_{26}O_{72}(OH)_3$ $\bullet H_2O$	9	McLemore et al. (2022)
*Sphalerite	Disseminated in Wind Mountain nepheline syenite and dikes	$(Zn,Fe)S$	na	Schreiner (1994), McLemore et al. (2022)
*Vitusite	Nepheline syenite Wind Mountain	$Na_3(Ce,La,Nd)(PO_4)_2$	34	McLemore et al. (2022)
*Xenotime	Nepheline syenite	$(Y,Th,U,Dy,Yb.Er,Gd)PO_4$	16 (48% Y)	McLemore et al. (2022)
*Zircon	Nepheline syenite, syenite	$ZrSiO_4$	4	Schreiner (1994)

DESCRIPTION OF MINERAL DEPOSITS AND ALTERATION

There are three types of REE-Nb-Zr mineral deposits in the Cornudas Mountains: (1) the basal unit (PEnsp2) of the Wind Mountain nepheline syenite laccolith, (2) syenite–phonolite and volcanic breccia dikes and plugs, and (3) skarns and carbonate-replacement deposits in Chess Draw and along the flanks of Wind Mountain. Mines, prospects, and mineralized zones are scattered throughout Chess Draw, Wind Mountain, and the McVeigh Hills, exposing the mineralized areas (McLemore et al., 2022).

Calcite veins are common in limestones near the mineralized skarns and intrusions and could be an exploration guide to mineralized zones. Evidence of contact metamorphism (skarns, carbonate-replacement deposits) is found throughout the Cornudas Mountains but is not extensive and is mostly concealed beneath boulders and alluvium eroding from the laccoliths and sills. Even in drill core, alteration zones are typically less than 1 m thick. The limestones west of Cornudas Mountain and along the contact with the Wind Mountain nepheline syenite are locally recrystallized to marble or green skarn or unmineralized tactite (metasomatized shale or siltstone). Skarns containing calc-silicate minerals are rare, but local narrow bands of aegirine, riebeckite, analcime, calcite, dolomite, and local eudialyte border many dikes and form small skarns. Locally, the skarns and contact-replacement deposits are of economic interest because they contain eudialyte that contains significant concentrations of Zr and REE.

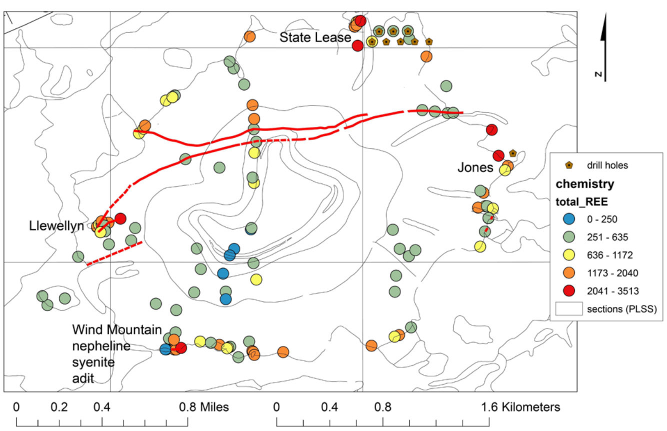

FIGURE 5. Map of Wind Mountain, showing the spatial distribution of total REE concentrations. See McLemore et al. (2022) for description of the geology (gray lines) and chemical analyses. Red lines = phonolite dikes.

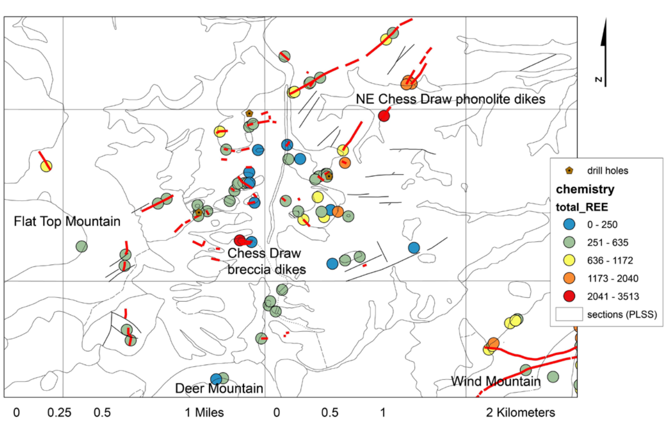

FIGURE 6. Map of Chess Draw area, showing the spatial distribution of total REE concentrations. See McLemore et al. (2022) for description of the geology (gray lines) and chemical analyses. Red lines = dikes.

REE-ZR-NB ECONOMIC POTENTIAL

Mineralogy

Several mineral species in the Cornudas Mountains host REE, Zr, and Nb (summarized in Table 4; McLemore et al., 2022). Trace amounts of galena, sphalerite, and molybdenite are found in the Cornudas Mountains; however, these minerals are not found in economic concentrations. Rheniite (ReS_2) was tentatively identified by electron microprobe but requires additional verification. Rhenium (Re) is a critical mineral typically found associated with molybdenite.

The predominant REE-Zr mineral in the Cornudas Mountains is eudialyte, which is found as red-to-pink to red-brown disseminations, cavity fillings, and veins in nepheline syenite, phonolite, skarns, and altered limestones in Chess Draw and along the flanks of Wind Mountain. Eudialyte is a group of minerals (Johnsen et al., 2003), and three species have been identified at Wind Mountain and Chess Draw: aqualite, magano-eudialyte, and sergevanite (Table 4). A eudialyte concentrate can be obtained by magnetic or flotation techniques (Vaccarezza and Anderson, 2019). REE can be recovered from eudialyte concentrates by acid leaching (Ma et al., 2019; Vaccarezza and Anderson, 2019).

Catapleiite is a red-brown hydrated zirconosilicate that also contains REE. This mineral forms a solid solution series with calciocatapleiite, both of which have been found at Wind Mountain. Catapleiite can be separated along with eudialyte by magnetic or flotation techniques (Silin et al., 2022).

Fine-grained REE fluorocarbonate minerals, predominantly bastnäsite-(Ce) with minor parisite-(Ce) are found disseminated in nepheline syenite at Wind Mountain. Other REE-bearing minerals found in the Wind Mountain and Chess Draw areas include monazite, xenotime, vitusite, and zircon. Metallurgical testing is required to determine if these minerals can be easily separated.

Pyrochlore is the predominant Nb mineral. Oxynatropyrochlore is locally present.

The only beryllium mineral found in the Cornudas Mountains is epididymite. Beryllium is a light element and difficult to identify by electron microprobe. The highest whole-rock concentration of Be in the Cornudas Mountains is 147 ppm (McLemore et al., 2022). Even though early exploration for Be occurred in the Cornudas Mountains, there is no evidence of economic concentrations in the area.

REE Potential in Wind Mountain

The basal unit (PEnsp2) of Wind Mountain laccolith has high potential for Zr, REE, and Nb (Fig. 5; McLemore et al., 2022). REE minerals are found in nepheline syenite, phonolite dikes, and skarns. Additional sampling and drilling are needed to locate REE-rich bodies with high enough REE, Nb, and Zr concentrations and tonnage to be economic. None of the other intrusions, outside of Chess Draw and Wind Mountain, have elevated REE, Zr, or Nb concentrations. Another potential mineral resource is nepheline syenite for use as ceramics, glass, or other industrial use (McLemore et al., 1994; McLemore and Guilinger, 1996).

REE Potential in Chess Draw

New mapping and geochemical sampling in Chess Draw (McLemore et al., 2022) indicates the aeromagnetic anomalies (Bultman, 2021a, b, 2022) could be the top of syenite and phonolite intrusions, possibly as laccoliths or plugs. The REE, Zr, and Nb potential in Chess Draw is high (Fig. 6), but drilling is required to locate specific areas of economic potential.

CONCLUSIONS

$^{40}Ar/^{39}Ar$ geochronology results indicate emplacement of igneous intrusions in two pulses in the Cornudas Mountains, from 37.14–34.5 and 32.48–26.95 Ma, spanning a longer interval than recorded by the previously published K/Ar ages (36.0–31.6 Ma). There are no significant differences in composition between the intrusions. REE, Zr, and Nb have the highest potential in the Wind Mountain and Chess Draw areas, specifically the PEnsp2 portion of the Wind Mountain laccolith (basal unit), phonolite and breccia dikes, and hydrothermal skarns and altered areas. The spatial distribution of REE, Zr, and Nb concentrations is discontinuous and localized. New drilling in the Chess Draw, along the contact of Wind Mountain, and in the McVeigh Hills is required to determine if there are zones enriched in REE, Zr, and Nb for economic development. Although the REE concentrations of the Wind Mountain and Chess Draw intrusions and altered areas are below normal economic grades (i.e., <5% total REE), eudialyte and other REE-minerals could be concentrated using magnetic separation and then REE could be leached. Chess Draw samples have higher Nb concentrations than Wind Mountain samples, whereas Wind Mountain samples have higher Zr concentrations. Pyrochlore is the predominant Nb mineral, and zircon and eudialyte are the predominant Zr minerals. None of the other intrusions, outside of Chess Draw and Wind Mountain, have elevated REE (>800 ppm), Zr, or Nb concentrations. Geophysical anomalies in Chess Draw and McVeigh Hills suggest presence of buried intrusions that could be sources of additional REE, Zr, or Nb concentrations.

ACKNOWLEDGMENTS

This work is part of ongoing research of the economic geology of mineral resources in New Mexico at NMBGMR, Nelia Dunbar, Director and State Geologist. This study was partially funded by the U.S. Geological Survey (USGS) Earth MRI Cooperative Agreement No. G20AC00170 and student grants from NMGS and New Mexico Tech Bright Star Scholarship. A special thanks to Bobby Jones, local rancher, for his assistance throughout the fieldwork. Geochemical analyses by U.S. Borax and Geovic-JS Group geologists provided additional analyses for interpretation. Geovic-JS Group allowed access to their core for logging and sampling. Discussions and field time with USGS geophysicists Mark Bultman and Mark Gettings were invaluable and appreciated. Virgil Lueth and Kelsey McNamara performed the XRD analyses. Peter Lyons, Stellah Cherotich, Ernest Brakohiapa, and other members of the Economic Geology Group at NMBGMR provided technical support. Dave Kasefang, Mark Leo-Russell, and Brandon Dennis provided database and other computer support. I would like to thank Russ Schreiner for his previous work in the area and sharing his insights and information over the years. Bonnie Frey and Shari Kelley reviewed an earlier version of this manuscript, and their comments are appreciated. Finally, James McLemore spent many days in the field camping, driving, mapping, and collecting samples with the senior author. Everyone's assistance is appreciated.

REFERENCES

Barker, D.S., 1977, Northern Trans-Pecos magmatic province: Introduction and comparison with the Kenya rift: Geological Society of America Bulletin, v. 88, p. 1421–1427, https://doi.org/10.1130/0016-7606(1977)88<1421:NTMPIA>2.0.CO;2.

Barker, D.S., 1987, Tertiary alkaline magmatism in Trans-Pecos Texas, *in* Fitton, J.G., and Upton, B.G.J., eds., Alkaline igneous rocks: Geological Society, Special Publication 30, p. 415–431, https://doi.org/10.1144/GSL.SP.1987.030.01.20.

Barker, D.S., and Hodges, F.N., 1977, Mineralogy of intrusions in the Diablo Plateau, northern Trans-Pecos magmatic province, Texas and New Mexico: Geological Society of America Bulletin, v. 88, p. 1428–1436, https://doi.org/10.1130/0016-7606(1977)88<1428:MOIITD>2.0.CO;2.

Barker, D.S., Long, L.E., Hoops, G.K., and Hodges, F.N., 1977, Petrology and Rb-Sr isotope geochemistry of intrusions in the Diablo Plateau, northern Trans-Pecos magmatic province, Texas and New Mexico: Geological Society America Bulletin, v. 88, p. 1437–1446, https://doi.org/10.1130/0016-7606(1977)88<1437:PARIGO>2.0.CO;2.

Boggs, R.C., 1985, Mineralogy of the Wind Mountain laccolith, Otero County, New Mexico [abs.]: New Mexico Geology, v. 7, p. 41–42.

Boggs, R.C., 1987, Mineralogy and textures of a eudialyte-bearing dike, Wind Mountain, Otero County, New Mexico [abs.]: New Mexico Geology, v. 9, p. 22.

Boggs, R.C., and Ghose, S., 1985, Georgechaoite, $NaKZrSi_3O_9 \cdot 2H_2O$, a new species from Wind Mountain, New Mexico: Canadian Mineralogist, v. 23, p. 1–4.

Bultman, M.W., 2021a, Aeromagnetic and aeroradiometric data acquired over parts of the Trans-Pecos region of west Texas and Southern New Mexico: U.S. Geological Survey data release, https://doi.org/10.5066/P91GTPQL.

Bultman, M.W., 2021b, Potential for concealed critical mineral deposits in the northern Trans-Pecos region of west Texas and southern New Mexico from a new aeromagnetic survey [abs.], *in* Critical minerals: From discovery to supply chain: Program with abstracts, British Columbia Ministry of Energy, Mines and Low Carbon Innovation, British Columbia Geological Survey GeoFile 2021-14, p. 46–47.

Bultman, M.W., 2022, Delineating potential for concealed critical mineral deposits in the northern Trans-Pecos region of west Texas and Southern New Mexico with a new aeromagnetic/aeroradiometric survey: Geological Society of Nevada Symposium, May 2–5.

Clabaugh, S.E., 1941, Geology of the northwestern portion of the Cornudas Mountains, New Mexico [M.S. thesis]: Austin, University of Texas, 66 p.

Clabaugh, S.E., 1950, Eudialyte and eucolite from southern New Mexico [abs.]: American Mineralogist, v. 35, p. 279–280.

Committee on Critical Mineral Impacts of the U.S. Economy, 2008, Minerals, Critical Minerals, and the U.S. Economy: Committee on Earth Resources, National Research Council, 264 p., http://www.nap.edu/catalog/12034.html.

DeMark, R.S., 1989, Micromounting in New Mexico: The Mineralogical Record, v. 20, p. 64.

Frost, B.D., Barnes, C.G., Collins, W.J., Arculus, R.J., Ellis, D.J., and Frost, C.D., 2001, A geochemical classification for granitic rocks: Journal of Petrology, v. 42, no. 11, p. 2033–2048, https://doi.org/10.1093/petrology/42.11.2033.

Ghose, S., and Thakur, P., 1985, The crystal structure of georgechaoite $NaKZrSi_3O_9 \cdot 2H_2O$: Canadian Mineralogist, v. 23, p. 5–10.

Johnsen, O., Ferraris, G., Gault, R.A., Grice, J.D., Kampf, A.R., and Pekov, I.V., 2003, The nomenclature of eudialyte-group minerals: Canadian Mineralogist, v. 41, p. 785–794, https://doi.org/10.2113/gscanmin.41.3.785.

King, W.E., and Harder, V.M., 1985, Oil and gas potential of the Tularosa Basin-Otero platform-Salt Basin graben area, New Mexico and Texas: New Mexico Bureau of Mines and Mineral Resources, Circular 198, 36 p.

Ma, Y., Stopic, S., and Friedrich, B., 2019, Hydrometallurgical treatment of an eudialyte concentrate for preparation of rare earth carbonate: Johnson Matthey Technology Review, v. 63, 12 p., https://doi.org/10.1595/205651318X15270000571362.

McLemore, V.T., 1996, Great Plains Margin (alkalic-related) gold deposits in New Mexico, *in* Cyner, A.R., and Fahey, P.L., eds., Geology and ore deposits of the American Cordillera: Geological Society of Nevada Symposium Proceedings, Reno/Sparks, Nevada, April 1995, p. 935–950.

McLemore, V.T., 2014, Rare Earth Elements Deposits in New Mexico, *in* Conway, F.M., ed., Proceedings of the 48th Annual Forum on the Geology of Industrial Minerals, Phoenix, Arizona, April 30–May 4, 2012: Arizona Geological Survey Special Paper #9, Chapter 3, p. 1–16, http://repository.azgs.az.gov/uri_gin/azgs/dlio/1568.

McLemore, V.T., 2018, Rare Earth Elements (REE) Deposits Associated with Great Plain Margin Deposits (Alkaline-Related), Southwestern United States and Eastern Mexico: Resources, v. 7, no. 1, 44 p., https://doi.org/10.3390/resources7010008.

McLemore, V.T., and Guilinger, J.R., 1993, Geology and mineral resources of the Cornudas Mountains, Otero County, New Mexico and Hudspeth County, Texas: New Mexico Geological Society, Guidebook 44, p. 145–154, https://doi.org/10.56577/FFC-44.145.

McLemore, V.T., and Guilinger, J.R., 1996, Industrial specifications of the Wind Mountain nepheline-syenite deposit, Cornudas Mountains, Otero County, New Mexico, *in* Austin, G.S., Barker, J.M., Hoffman, G., Gilson, N., and Zidec, J., eds., Proceedings of the 31st Forum on the Geology of Industrial Minerals, Borderland Forum: New Mexico Bureau of Mines and Mineral Resources, Bulletin 154, p. 121–126.

McLemore, V.T., and Gysi, A., 2023, Critical minerals in New Mexico: Earth Matters, winter, in press.

McLemore, V.T., Guilinger, J.R., and Oumiette, M.A., 1994, Geology of the Wind Mountain nepheline syenite deposit, Cornudas Mountains, Otero County, New Mexico: Society Mining, Metallurgy, and Exploration, Preprint 94-63, 10 p.

McLemore, V.T., Iverson, N., Woodard, M., Attia, S., Dietz, H., Owen, E., Haft, E.B., Childress, T., Trivitt, A., and Kelley, R., 2022, Geology and mineral deposits of the Cornudas Mountains, Otero County, New Mexico: New Mexico Bureau of Geology and Minerals Resources, Open-File Report 619, 151 p.

McLemore, V.T., Haft, E., Owen, E., Woodard, M., and Iverson, N., 2023, Mineralogy and Geochemistry of Selected Rare Earth Elements (REE) Deposits in the North American Cordilleran alkaline-igneous belt in New Mexico: Minexchange, 2023 SME Annual Conference Technical Program, preprint, 13 p.

Michayluk, M.C., and Cone, J., 2017a, Collecting Wind Mountain (in the Cornudas Mountains, NM, USA): part 1, https://www.mindat.org/a/windmountain_pt1.

Michayluk, M.C., and Cone, J., 2017b, Collecting Wind Mountain (in the Cornudas Mountains, NM, USA): part 2, https://www.mindat.org/a/windmountain_pt2.

Mutschler, F.E., Griffin, M.E., Stevens, D.S., and Shannon, S.S., Jr., 1985, Precious metal deposits related to alkaline rocks in the North American Cordillera—an interpretive review: Transactions Geological Society of America, v. 88, p. 355–377.

Mutschler, F.E., Mooney, T.C., and Johnson, D.C., 1991, Precious metal deposits related to alkaline igneous rocks: a space-time trip through the Cordillera: Mining Engineering, v. 43, p. 304–309.

Nutt, C.J., and O'Neill, J.M., 1998, Geologic framework of Tertiary intrusions of the Cornudas Mountains, southern New Mexico: New Mexico Geological Society, Guidebook 49, p. 129–134, https://doi.org/10.56577/FFC-49.129.

Nutt, C.J., O'Neill, J.M., Kleinkopf, M.D., Klein, D.P., Miller, W.R., Rodriquez, B.D., and McLemore, V.T., 1997, Geology and mineral resources of the Cornudas Mountains, New Mexico: U.S. Geological Survey, Open-File Report 97-282, 46 p., https://doi.org/10.3133/ofr97282.

O'Neill, J.M., and Nutt, C.J., 1998, Geologic map of the Cornudas Mountains, Otero County, New Mexico: U.S. Geological Survey, Miscellaneous Geologic Investigations Map, I-2631, scale 1:24,000.

Owen, E.J., and McLemore, V.T., 2023, Pre-conference Field Trip Two: Cornudas Mountains: New Mexico Geological Society, this guidebook.

Potter, L.S., 1996a, Chemical variation along strike in feldspathoidal rocks of the eastern alkali belt, Trans-Pecos magmatic province, Texas and New Mexico: The Canadian Mineralogist, v. 34, p. 241–264.

Potter, L.S., 1996b, Chemical and isotopic variation along strike in the eastern alkali belt, Trans-Pecos magmatic province, Texas and New Mexico [Ph.D. dissertation]: Austin, University of Texas, 267 p.

Schreiner, R.A., 1994, Mineral investigation of Wind Mountain and the Chess Draw area, Cornudas Mountains, Otero County, New Mexico: U.S. Bureau of Mines, MLA 26-94, 51 p.

Silin, I., Gürsel, D., Bütchter, C., Weitkämper, L. and Wotruba, H., 2022, Recovery of catapleiite and eudialyte from non-magnetic fraction of eudialyte ore processing of Norra Karr deposit: Minerals, v. 12, 19 p., https://doi.org/10.3390/min12010019.

Timm, B.C., 1941, The geology of the southern Cornudas Mountains, Texas and New Mexico [M.S. thesis]: Austin, University of Texas, 55 p.

U.S. Borax, 1986, Geologic map of Chess Draw: unpublished map, NMBGMR file data.

Vaccarezza, V., and Anderson, C., 2019, An overview of beneficiation and hydrometallurgical techniques on eudialyte group minerals: Mining, Metallurgy, and Exploration, v. 37, p. 39–50, https://doi.org/10.1007/s42461-019-00132-5.

Warner, L.A., Holser, W.T., Wilmarth, V.R., and Cameron, E.N., 1959, Occurrence of nonpegmatite beryllium in the United States: U.S. Geological Survey, Professional Paper, v. 318, 198 p., https://doi.org/10.3133/pp318.

Zapp, A.D., 1941, Geology of the northeastern Cornudas Mountains, New Mexico [M.S. thesis]: Austin, University of Texas, 63 p.

Pump jack in sinkhole, Dagger Draw oil field, Eddy Co., NM.